

BIROn - Birkbeck Institutional Research Online

Crawford, Ian (2000) A study of interstellar Na I D absorption lines towards the Lupus molecular clouds. *Monthly Notices of the Royal Astronomical Society* 317 (4), pp. 996-1004. ISSN 0035-8711.

Downloaded from: <https://eprints.bbk.ac.uk/id/eprint/28527/>

Usage Guidelines:

Please refer to usage guidelines at <https://eprints.bbk.ac.uk/policies.html>
contact lib-eprints@bbk.ac.uk.

or alternatively

A study of interstellar Na I D absorption lines towards the Lupus molecular clouds

I. A. Crawford[★]

Department of Physics and Astronomy, University College London, Gower Street, London WC1E 6BT

Accepted 2000 May 22. Received 2000 May 10; in original form 2000 March 21

ABSTRACT

Intermediate-resolution ($60\,000 \leq R \leq 120\,000$) observations of interstellar Na I lines towards 29 stars in the general direction of the Lupus molecular clouds ($330^\circ \leq l \leq 350^\circ$; $0^\circ \leq b \leq 25^\circ$) are presented. Previously published spectra towards an additional seven stars are also included. Based on the *Hipparcos* distances to these stars, and the minimum distance at which strong interstellar Na I lines appear in the spectra, I obtain a distance of $\sim 150 \pm 10$ pc to the Lupus molecular complex. While in agreement with a number of other independent estimates, this result is at odds with the value of 100 pc recently obtained by Knude & Høg from a *Hipparcos*-based study of interstellar extinction. A possible explanation for this discrepancy is discussed, and it is concluded that the value of 150 ± 10 pc obtained here is to be preferred. In addition, these observations have some other implications for the structure of the interstellar medium in this direction, and these are briefly considered.

Key words: line: profiles – ISM: clouds – ISM: individual: Lupus – ISM: structure.

1 INTRODUCTION

The Lupus molecular clouds ($330^\circ \leq l \leq 350^\circ$; $0^\circ \leq b \leq 25^\circ$) form part of a roughly 1-kpc long ridge of molecular clouds extending from Vela to Cygnus, and which may delineate the inner edge of the Local spiral arm (Dame et al. 1987). Other components of this large-scale interstellar structure include, in order of increasing Galactic longitude, the Chamaeleon clouds ($l \approx 300^\circ$), the Southern Coalsack ($l \approx 305^\circ$) and the ρ Oph clouds ($l \approx 360^\circ$; cf. fig. 7 of Dame et al. 1987). At a slightly uncertain distance of ~ 150 pc (see below), the Lupus complex is one of the closest sites of low-mass star formation to the Sun (Krautter 1991, and references therein). This activity, as indicated by the distribution of T Tauri stars, is associated with a small number of dense, elongated, dark clouds ($\lesssim 2^\circ$ ($\lesssim 5$ pc) in size and designated Lupus 1 to 5 (Krautter 1991; Tachihara et al. 1996). Photographs of these regions have been presented by Krautter (1991), and they show up very clearly in the ^{13}CO ($J = 1 \rightarrow 0$) maps of Tachihara et al. (1996). These dense regions are embedded in a much larger, but more diffuse, volume of molecular gas mapped in ^{12}CO ($J = 1 \rightarrow 0$) by Murphy, Cohen & May (1986, their fig. 2), and which occupies a local standard of rest (LSR) velocity range from 0.0 to $+11.6 \text{ km s}^{-1}$.

Here, I report an observational study of interstellar Na I D absorption lines towards 29 early-type (B and A) stars in the same region of sky as the Lupus molecular clouds. Most of these stars are members of the Sco-Cen OB association, which also lies at a

distance of about 150 pc, and in its entirety occupies the Galactic longitude range $290^\circ \leq l \leq 360^\circ$ (de Geus, de Zeeuw & Lub 1989). The main aim was to determine the distance to the Lupus molecular clouds by searching for interstellar lines in the spectra of stars at a range of known distances. This approach offers significant advantages over methods that rely solely on the distribution of interstellar extinction, for while the latter are sensitive only to the total quantity of intervening matter, absorption lines provide additional information on the velocity structure, and thus the number of discrete absorbing regions, present along a given line of sight. The observations were obtained during observing runs at Mt Stromlo Observatory in 1991 June, 1992 June and 1993 June, in anticipation of the astrometric distances to be obtained by the *Hipparcos* satellite. In the event, although *Hipparcos* was launched in 1989 August, the catalogue only became available in 1997 (Perryman et al. 1997; ESA 1997).

The stars observed are listed in Table 1, together with their V magnitudes, galactic coordinates and distances. With the exception of three cases where the *Hipparcos* errors were very large (owing to the parallax being close to the ~ 1 mas measurement limit), and one star not included in the catalogue, all distances are *Hipparcos* values (ESA 1997). The exceptions, identified in the table, are photometric distances obtained by de Geus et al. (1989). In addition, because they lie in the same area of sky, I have included in this study seven stars that were observed some years previously with the same instrument (Crawford 1991); Table 2 identifies these stars, and gives their *Hipparcos* distances, which supersede the photometric values tabulated in the earlier paper.

[★] E-mail: iac@star.ucl.ac.uk

Table 1. Summary of the observational data. The first five columns give the HD number, visual magnitude, galactic coordinates and distance of each star (unless noted in the footnotes to the table, all distances are from the *Hipparcos* catalogue); Det, ΔV and Exp identify the detector, spectral resolution (FWHM) and exposure time, respectively; $W_\lambda(D_2)$ and $W_\lambda(D_1)$ are the equivalent widths of the two Na I D lines; and V_{LSR} , b and $\log N$ give the LSR radial velocity, velocity dispersion and column density of each detected absorption component (see text for details).

Star (HD)	V	Long ($^\circ$)	Lat ($^\circ$)	Dist (pc)	Det. (ΔV) (km s $^{-1}$)	Exp (s)	$W_\lambda(D_2)$ (mÅ)	$W_\lambda(D_1)$ (mÅ)	V_{LSR} (km s $^{-1}$)	b (km s $^{-1}$)	$\log N$ (cm $^{-2}$)
133716	7.2	330.4	+17.6	160 $^{+31}_{-22}$	CCD (3.9)	1000	≤ 10	≤ 10	≤ 10.71
134685	7.7	333.0	+19.5	174 $^{+36}_{-26}$	PCA (5.0)	3600	85 ± 9 127 ± 8	-10.2 ± 0.4 +5.9 ± 0.2	3.0 $^{+1.0}_{-1.0}$ 2.0 $^{+0.5}_{-1.3}$	11.70 $^{+0.10}_{-0.05}$ 12.30 $^{+2.00}_{-0.15}$
136298	3.2	331.3	+13.8	156 $^{+24}_{-19}$	PCA (2.5)	1500	≤ 3.4	≤ 10.24
136664	4.5	333.8	+16.8	186 $^{+31}_{-23}$	PCA (2.5)	2600	≤ 6.5	≤ 10.52
136961	6.8	334.7	+17.3	148 $^{+22}_{-17}$	PCA (5.0)	3600	23 ± 5	-14.3 ± 0.9	4.0 $^{+1.5}_{-2.0}$	11.10 $^{+0.10}_{-0.10}$
137169	9.0	332.1	+13.4	475 a	CCD (3.9)	1000	106 ± 26	74 ± 24	+9.7 ± 1.9	5.0 $^{+3.0}_{-2.0}$	11.80 $^{+0.20}_{-0.30}$
137432	5.4	334.6	+16.3	128 $^{+16}_{-13}$	PCA (2.5)	3600	≤ 6.9	≤ 10.55
137957	7.4	330.0	+8.9	198 $^{+43}_{-30}$	PCA (5.0)	6400	112 ± 9 100 ± 9	+4.5 ± 0.2 +15.4 ± 0.3	1.8 $^{+0.7}_{-1.1}$ 1.8 $^{+0.7}_{-1.3}$	12.30 $^{+1.70}_{-0.15}$ 12.10 $^{+1.90}_{-0.15}$
138138	6.9	337.1	+18.2	100 $^{+11}_{-9}$	CCD (5.0)	1000	25 ± 4	19 ± 4	-12.0 ± 0.6	4.0 $^{+1.5}_{-1.0}$	11.20 $^{+0.15}_{-0.10}$
139094	7.4	343.0	+23.2	289 $^{+126}_{-67}$	PCA (5.0)	1500	330 ± 12	...	-3.1 ± 0.3	3.0 $^{+2.5}_{-0.7}$	14.60 $^{+0.70}_{-1.60}$
139233	6.6	335.0	+13.1	196 $^{+38}_{-28}$	PCA (5.0)	2500	≤ 6.1	≤ 10.50
139524	8.1	332.1	+8.9	424 a	PCA (5.0)	3600	151 ± 8 16 ± 6	+4.5 ± 0.2 +17.5 ± 1.1	2.5 $^{+1.0}_{-1.9}$ ≤ 4.0	12.40 $^{+2.40}_{-0.20}$ 11.10 $^{+0.10}_{-0.20}$
140008	4.7	338.5	+16.1	121 $^{+14}_{-11}$	PCA (5.0)	1800	≤ 2.5	≤ 10.11
140475	7.7	338.6	+15.5	125 $^{+19}_{-15}$	PCA (5.0)	3600	≤ 18	≤ 10.97
140602	8.3	333.1	+8.3	173 $^{+36}_{-26}$	PCA (5.0)	3600	≤ 7.6	≤ 10.59
140784	5.6	339.2	+15.6	119 $^{+15}_{-12}$	PCA (5.0)	2400	≤ 4.1	≤ 10.33
140817	6.8	338.7	+14.9	131 $^{+36}_{-23}$	CCD (5.0)	3600	≤ 4.5	≤ 4.5	≤ 10.37
141180	8.3	344.4	+20.7	358 a	PCA (5.0)	3600	92 ± 12 56 ± 10 68 ± 10	-9.3 ± 0.5 +1.7 ± 0.5 +17.8 ± 0.4	3.0 $^{+1.0}_{-1.0}$ ≤ 3.0 ≤ 3.5	11.80 $^{+0.05}_{-0.10}$ 11.65 $^{+1.35}_{-0.10}$ 11.70 $^{+1.30}_{-0.10}$
141905	8.3	336.7	+10.8	204 $^{+48}_{-33}$	PCA (5.0)	3600	216 ± 21	...	+5.6 ± 0.5	2.2 $^{+1.3}_{-0.7}$	14.00 $^{+0.70}_{-1.00}$
142201	10.5	336.8	+10.4	625 a	CCD (5.0)	3000	58 ± 17 350 ± 16	30 ± 14 312 ± 15	-21.0 ± 4.0 +9.3 ± 0.4	10.0 $^{+3.0}_{-3.0}$ 4.7 $^{+1.5}_{-2.2}$	11.53 $^{+0.10}_{-0.20}$ 13.23 $^{+2.10}_{-0.36}$
142431	7.0	336.6	+9.8	119 $^{+13}_{-11}$	PCA (5.0)	4800	≤ 11	≤ 10.75
143118	3.4	338.8	+11.0	151 $^{+20}_{-16}$	PCA (2.5)	1800	≤ 4.1	≤ 10.33
143927	7.1	339.9	+10.8	146 $^{+22}_{-17}$	PCA (5.0)	3600	112 ± 6	...	+4.8 ± 0.2	2.0 $^{+1.0}_{-1.4}$	12.30 $^{+2.20}_{-0.20}$
144294	4.2	340.8	+11.3	126 $^{+15}_{-12}$	PCA (2.5)	1800	≤ 6.4	≤ 10.52
145102	6.6	348.6	+17.9	175 $^{+31}_{-23}$	CCD (5.0)	1000	76M ± 8 195 ± 9	49 ± 6 137 ± 7	-12.0 ± 0.3 +3.8 ± 0.3	≤ 4.0 5.0 $^{+1.0}_{-1.5}$	11.83 $^{+0.10}_{-0.14}$ 12.34 $^{+0.11}_{-0.20}$
146284	6.7	351.6	+18.7	264 $^{+90}_{-53}$	CCD (5.0)	1000	81 ± 6 186 ± 6	53 ± 5 141 ± 5	-14.2 ± 0.3 +1.6 ± 0.2	3.5 $^{+1.0}_{-1.0}$ 4.0 $^{+1.0}_{-1.0}$	11.80 $^{+0.10}_{-0.10}$ 12.42 $^{+0.10}_{-0.12}$
146332	7.7	347.5	+14.9	626 a	PCA (5.0)	3600	319 ± 25	...	+4.3 ± 0.7	3.5 $^{+2.0}_{-1.5}$	13.70 $^{+1.50}_{-0.90}$

Table 1 – *continued*

Star (HD)	<i>V</i>	Long (°)	Lat (°)	Dist (pc)	Det. (ΔV) (km s ⁻¹)	Exp (s)	$W_\lambda(D_2)$ (mÅ)	$W_\lambda(D_1)$ (mÅ)	V_{LSR} (km s ⁻¹)	<i>b</i> (km s ⁻¹)	log <i>N</i> (cm ⁻²)
148199	7.0	349.5	+13.5	151 ⁺²⁵ ₋₁₉	CCD (5.0)	1000	227±6	176±5	+2.0±0.2	4.1 ^{+0.5} _{-0.5}	12.55 ^{+0.10} _{-0.10}
148594	6.9	350.9	+13.9	167 ⁺²⁸ ₋₂₁	CCD (5.0)	1000	171±5	148±5	+3.9±0.2	2.4 ^{+0.6} _{-0.5}	12.73 ^{+0.20} _{-0.30}

^a Photometric distances from de Geus et al. (1989).^b Upper limit to log *N* obtained by assuming *b* > 0.3 km s⁻¹ (see text).

Fig. 1 shows the locations of all these stars on the sky, and the location of the Lupus molecular cloud complex as delineated by the outer (1.5 K km s⁻¹) CO contour obtained by Murphy et al. (1986).

2 OBSERVATIONS AND REDUCTIONS

All observations were obtained using the coudé echelle spectrograph of the Mt Stromlo 74-inch (1.9-m) telescope. Two camera/detector combinations were employed: the 130-inch focal length camera with the Mt Stromlo Photon Counting Array detector (PCA; Stapinski, Rodgers & Ellis 1981), and the 32-inch focal length camera with a GEC 578×385 (22-μm) pixel charge-coupled device (CCD). These different camera/detector combinations, together with different choices of slit width, have resulted in spectral resolutions, *R*, in the range 60 000 to 120 000 [5.0 to 2.5 km s⁻¹ full width at half-maximum (FWHM)]; the resolution employed in each case is given in Table 1. Use of the shorter, 32-inch, camera resulted in both the D₂ (5889.951 Å) and D₁ (5895.924 Å) lines being recorded simultaneously, whereas the higher dispersion of the 130-inch camera only permitted observations of the D₂ line.

The spectra were extracted from the PCA and CCD images using the FIGARO data reduction package (Shortridge et al. 1998). Background light was extracted from the inter-order region and subtracted. The spectra were wavelength calibrated by means of a Th–Ar lamp; typical rms residuals to the arc lines were ≤0.002 Å (≤0.1 km s⁻¹). Strong atmospheric water lines occur in this region of the spectrum, and these were removed by dividing the object spectra by an atmospheric template spectrum as described by Crawford, Barlow & Blades (1989). To allow for night-to-night and zenith-distance variations in the atmospheric lines, in each case the template spectrum was scaled so that the optical depths of atmospheric lines in the template matched those in the object spectra not blended with the interstellar lines. Following division by the atmospheric template, the spectra were converted to the velocity frame defined by the kinematical LSR (Wallace & Clayton 1996).

For stars where no interstellar absorption was detected, Table 1 gives the two-sigma upper limits to the equivalent widths, and corresponding column densities. These are based on the continuum signal-to-noise ratio and appropriate spectral resolution, and the column density upper limits assume a linear (i.e. unsaturated) curve of growth.

Table 2. Stars previously observed towards the Lupus clouds (Crawford 1991). Notation is the same as for Table 1.

Star (HD)	Long (°)	Lat (°)	Dist (pc)	$W_\lambda(D_2)$ (mÅ)	V_{LSR} (km s ⁻¹)	<i>b</i> (km s ⁻¹)	log <i>N</i> (cm ⁻²)
138690	333.2	+11.9	174 ⁺⁴⁸ ₋₃₁	≤2.0	≤10.00
141637	346.1	+21.7	160 ⁺²⁷ ₋₂₀	218±18	-6.7 +1.0	2.7 ^{+0.3} _{-0.5} 1.6 ^{+0.7} _{-1.0}	12.04 ^{+0.07} _{-0.04} 12.38 ^{+1.92} _{-0.23}
142114	346.9	+21.6	133 ⁺²⁵ ₋₁₈	167±14	-8.1 -3.1	2.2 ^{+0.6} _{-1.0} ≤3.0	12.30 ^{+1.00} _{-0.12} 11.40 ^{+0.08} _{-0.22}
142669	344.6	+18.3	125 ⁺¹⁵ ₋₁₂	≤5.0	≤10.40
143699	339.1	+10.4	162 ⁺²³ ₋₁₈	≤5.0	≤10.40
148703	345.9	+9.2	229 ⁺⁵¹ ₋₃₅	152±13	-9.6 -1.1 +3.4 +12.4	≤2.5 ≤2.5 ≤3.0 5.0 ^{+1.0} _{-1.0}	11.08 ^{+0.03} _{-0.13} 12.00 ^{+2.30} _{-0.10} 11.18 ^{+0.30} _{-0.18} 10.90 ^{+0.10} _{-0.12}
151890	346.1	+3.9	252 ⁺¹⁰⁹ ₋₅₉	9.5±2.1	+0.5	≤1.0	10.85 ^{+0.03} _{-0.07}

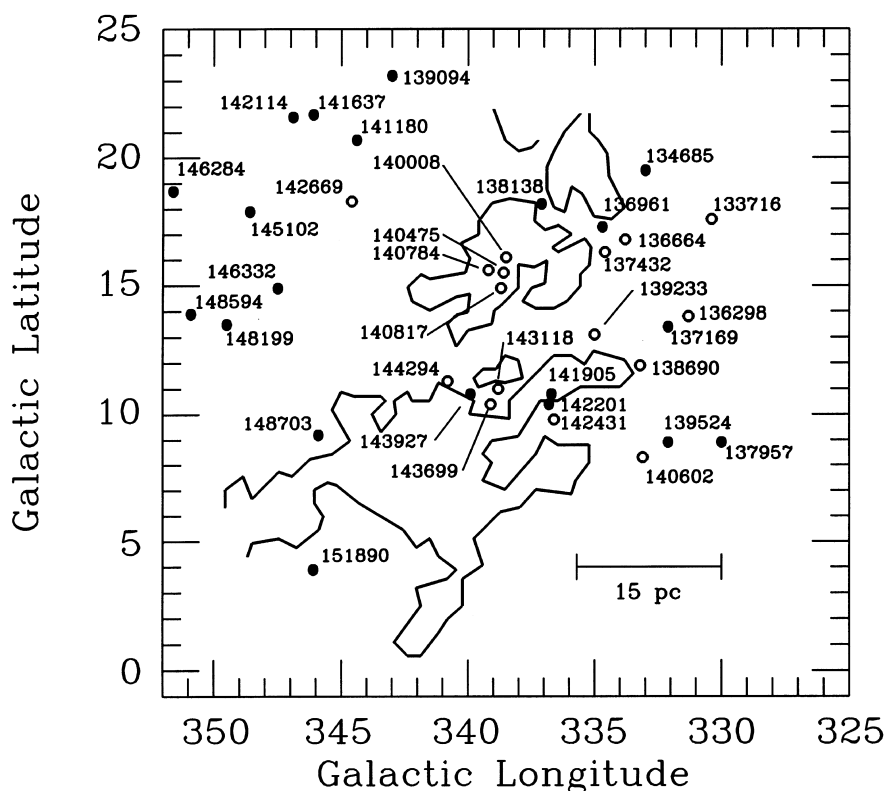


Figure 1. The locations of the stars observed relative to the outer (1.5 K km s^{-1}) ^{12}CO contours obtained for the Lupus clouds by Murphy et al. (1986); for the locations of the dense, star-forming, clumps within this region see the ^{13}CO map of Tachihara et al. (1996). Filled circles represent stars for which interstellar lines were detected, while open circles represent stars for which only upper limits were obtained. The scale bar assumes a distance of 150 pc (see text).

3 LINE PROFILE ANALYSIS

For stars where interstellar absorption components were detected, Table 1 gives the LSR velocity (V_{LSR}), velocity dispersion parameter (b) and column density ($\log N$) obtained using the interstellar line profile modelling routines in the DIPSO data analysis package (Howarth et al. 1998). For several target stars the interstellar lines were found to be superimposed on much broader stellar photospheric lines, the profiles of which provide the local continuum for the interstellar absorption. These stellar lines were fitted with Gaussian profiles and divided out prior to the line profile analysis. The observed spectra are compared with the results of the line profile analysis in Fig. 2. The relevant atomic data were taken from Morton (1991).

The velocity dispersions tabulated in Table 1 have been obtained after allowing for convolution with an instrumental function of FWHM ΔV (as given in column 7 of Table 1), and for the hyperfine structure present in the NaD lines. The latter amounts to a velocity splitting of 1.01 and 1.08 km s^{-1} for the D_2 and D_1 lines, respectively (e.g. Welty, Hobbs & Kulkarni 1994), and although unresolved here nevertheless broadens the line profiles. It will be seen that most of the b values listed in Table 2 lie in the range $2\text{--}5 \text{ km s}^{-1}$. As the lower end of this range is below the instrumental resolution, a brief discussion of their reliability and significance is appropriate.

The first point to note is that line profile modelling is insensitive to b values below the instrumental value of $b_{\text{inst}} \equiv \Delta V / 1.6651$ (or 3.0 km s^{-1} for $\Delta V = 5.0 \text{ km s}^{-1}$). This can make it difficult to determine a lower limit to b from the observed line profiles. For strong (saturated) lines it is possible to use the relationship

between b and N (low b implies large N , and vice versa) to obtain an *extreme* lower limit to b based on the non-appearance of broad damping wings in the observed profile. Several of the b value lower limits (and $\log N$ upper limits) listed in Table 1 have been obtained in this way; the resulting column densities can be uncertain by up to two orders of magnitude.

For lines where this method was unable to determine a realistic lower limit, an upper limit is recorded in Table 1. In two cases (indicated in the table) it was necessary to *assume* a lower limit of $b > 0.3 \text{ km s}^{-1}$, in order to obtain realistic upper limits to $\log N$; such a low value of b (corresponding to thermal broadening at 125 K in the absence of turbulence) is smaller than the lowest values typically reported in the literature on the basis of ultrahigh-resolution spectroscopy of interstellar clouds (see below). We note that for weak lines this uncertainty in b has little effect on the column densities, as for unsaturated lines N is independent of b .

While we can have some confidence in the *effective* b values listed in Table 1, these should not necessarily be interpreted as true velocity dispersions of actual interstellar clouds. A Na b value of 3.0 km s^{-1} would imply an implausibly high kinetic temperature ($1.2 \times 10^4 \text{ K}$) and/or significantly supersonic turbulence. It is much more likely that these relatively large b values mask unresolved velocity structure. Indeed, ultrahigh-resolution studies ($R \geq 600\,000$) routinely resolve apparently single interstellar Na lines into multiple components having intrinsic b values below 1.0 km s^{-1} (e.g. Welty et al. 1994; Barlow et al. 1995; Dunkin & Crawford 1999). Higher-resolution observations, preferably of an unsaturated line such as K I, would be required to determine the extent to which such unresolved velocity structure is present. Note

that, if it is, the column densities of affected components may have been underestimated (substantially so in the case of saturated lines).

Finally, we note that for the CCD observations, where both the Na D₁ and D₂ lines have been observed, the doublet ratio method could in principle be used to obtain independent estimates of b and N [see Somerville (1988) for a brief review of the method, although his procedure must be modified along the lines described by Hobbs (1969) in order to allow for the hyperfine structure]. In the event, however, it turned out that most of the lines were so heavily saturated (i.e. doublet ratios close to unity), and the errors on the equivalent widths so relatively large, that this method failed to yield better constraints on b and N than those obtained by the line profile method outlined above.

4 DISCUSSION

Fig. 3 shows a plot of the column density against stellar distance, for all velocity components identified towards those stars having *Hipparcos* distance determinations. In this diagram, components within the velocity range occupied by the molecular gas associated with the Lupus complex ($0 \leq V_{\text{LSR}} \leq 12 \text{ km s}^{-1}$; Murphy et al. 1986) are represented by filled circles. Components having negative LSR velocities are represented by open circles, and upper limits by open triangles. In this distance range only two stars (represented by crosses within a circle) exhibit absorption with LSR velocities more positive than the Lupus complex, although several of the more distant stars also exhibit such positive velocity components.

This diagram may now serve as a basis for further discussion.

4.1 The Lupus components

Fig. 3 shows that all but two of the absorption components occupying the Lupus complex velocity range (filled circles) have Na I column densities of $\log N \geq 12.00 \text{ cm}^{-2}$ (and line saturation means that several may have column densities up to two orders of magnitude higher), as would be expected for dense gas in the vicinity of molecular clouds. Two stars (HD 148703 and 151890) have velocity components within the Lupus complex velocity range, but with an order-of-magnitude lower column density (Table 2). Both of these are fairly distant stars ($D \approx 240 \text{ pc}$, albeit with fairly large errors) and, given their proximity to the CO emission contours (Fig. 1), these low column densities are surprising. Of these stars, HD 148703 does have a much stronger Na I absorption component at $V_{\text{LSR}} = -1.1 \text{ km s}^{-1}$, which is only marginally outside the Lupus velocity range, and which Crawford (1991) identified with the molecular complex on the basis of its low Na I/Ca II ratio. This would imply that the atomic gas associated with the Lupus complex extends to somewhat more negative velocities than the CO emission. This is consistent with the observation that the strongest absorption component plotted in Fig. 3 (that towards HD 139094) has an LSR velocity of -3.1 km s^{-1} , although in this case the star has a greater projected separation from the molecular emission. In any case, if the -1.1 km s^{-1} component towards HD 148703 does arise within the Lupus complex, the weaker $+3.4 \text{ km s}^{-1}$ component could then be interpreted either as arising in additional internal structure within the complex, or as unrelated foreground or background absorption. In the case of HD 151890 ($\mu^1 \text{ Sco}$), the detection of only one weak absorption component [cf. Table 2; also Hobbs (1978), who

obtained essentially the same values] implies that the ‘embayment’ around this star in the ^{12}CO map (Fig. 1) must also extend to any associated less dense material.

Regardless of these caveats, it is clear from Fig. 3 that none of the absorption components occupying the velocity range of the Lupus molecular clouds occur closer than 140 pc . As gas sufficiently dense to form CO would certainly be expected to show strong Na I absorption lines, this may be taken as a lower limit to the distance to the molecular gas in this direction. Allowing for the *Hipparcos* distance error estimates, the data presented in Fig. 3 suggest a distance of $\sim 150 \pm 10 \text{ pc}$ for the molecular clouds.

Previously published distance determinations have been discussed by Krautter (1991). Several of these relate to the distances of individual stars, especially those of the Herbig Ae/Be star HR 5999 and its close companion HR 6000 (Bessell & Eggen 1972; Schneider & Elmegreen 1979; Eggen 1983), which lie close to the centre of the Lupus 3 dark cloud (cf. fig. 2 of Krautter 1991). *Hipparcos* distances are now available for both these stars (parallaxes of 4.81 ± 0.87 and $4.15 \pm 0.83 \text{ mas}$, respectively), and a simple average yields $223^{+35}_{-26} \text{ pc}$. Clearly, as a Herbig Ae/Be star surrounded by T Tauri stars, the case for a physical association of HR 5999 with the Lupus dark clouds is very strong. Other bright stars thought to be physically close to the molecular clouds include HD 140784 (Appenzeller, Mundt & Wolf 1978), and HD 143927 and 149447 (Schneider & Elmegreen 1979) [note that Krautter’s (1991) discussion contains a number of typographical errors in these HD numbers]. However, with the exception of HD 143927, which is clearly associated with a reflection nebula (and here found to have a strong absorption component at the expected velocity), a visual inspection of the ESO Digitized Sky Survey (<http://archive.eso.org/dss/dss>) fails to show a convincing relationship between the other stars and dense interstellar matter; certainly, the lack of interstellar Na I absorption towards HD 140784 (Table 1) indicates that this star at least must lie in the foreground. Other, more statistically meaningful, distance estimates for the Lupus clouds have been obtained by photometric studies of interstellar reddening towards much larger samples of stars. Using these methods, Franco (1990) obtained a value of $165 \pm 15 \text{ pc}$; Hughes, Hartigan & Clampitt (1993) obtained $140 \pm 20 \text{ pc}$; and Knude & Høg (1998) obtained 100 pc . These various distance measurements, together with that obtained here, are summarized in Table 3.

The value of $150 \pm 10 \text{ pc}$ obtained in the present work is in good agreement with three out of the five previous measurements reported in Table 3. It is surprising that the *Hipparcos* distances place HR 5999 and 6000 at a significantly greater distance than the molecular clouds, and further studies would seem justified to verify this. It is even more surprising that the recent study of interstellar reddening by Knude & Høg (1998), itself based on *Hipparcos* data, should have concluded that the distance to the Lupus complex is as low as 100 pc . Given that, on the basis of their revised distance, Knude & Høg suggest reducing the luminosities of young stellar objects associated with the complex by a factor of 2, it is important to determine whether or not they have a persuasive case.

Clearly, the data presented in Fig. 3 do not support a distance as low as 100 pc . It could perhaps be argued that Knude & Høg included many more stars in their study, and that the rather sparse coverage over much of the region in the present study means that this conclusion is premature. However, the present observations do have a reasonable coverage in the vicinity of several of the densest

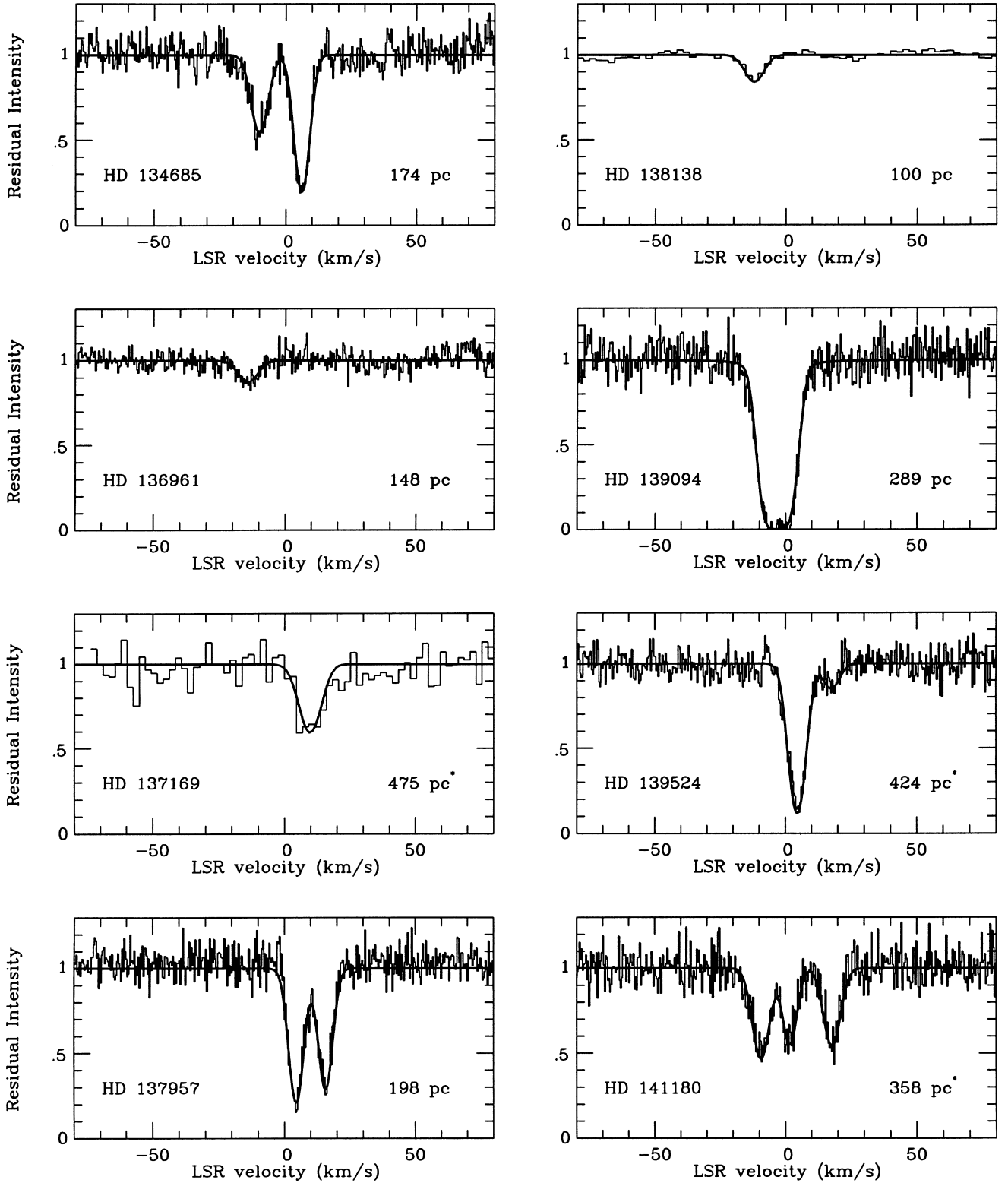


Figure 2. The interstellar Na D₂ lines towards the observed stars. The observed data are plotted as histograms, and the theoretical line profiles with the parameters given in Table 1 are shown superimposed. Distances are from *Hipparcos*, unless marked *, in which case they are less certain photometric values (Table 1).

parts of the Lupus complex. In particular, in the region of Lupus 1 ($l \approx 339^\circ$, $b \approx +15^\circ$ to $+17.5^\circ$; cf. fig. 1 of Tachihara et al. 1996), four stars (HD 140008, 140475, 140784 and 140817) lie within 1° of the molecular emission. These four stars can easily be identified

in fig. 1(a) of Krautter (1991; see also ESO Sky Survey field 388), where it will be seen that they lie *between* the densest regions of optical extinction (named Lupus 1N and Lupus 1S by Krautter 1991). Note that 1° projects to only 2.6 pc for a distance of 150 pc,

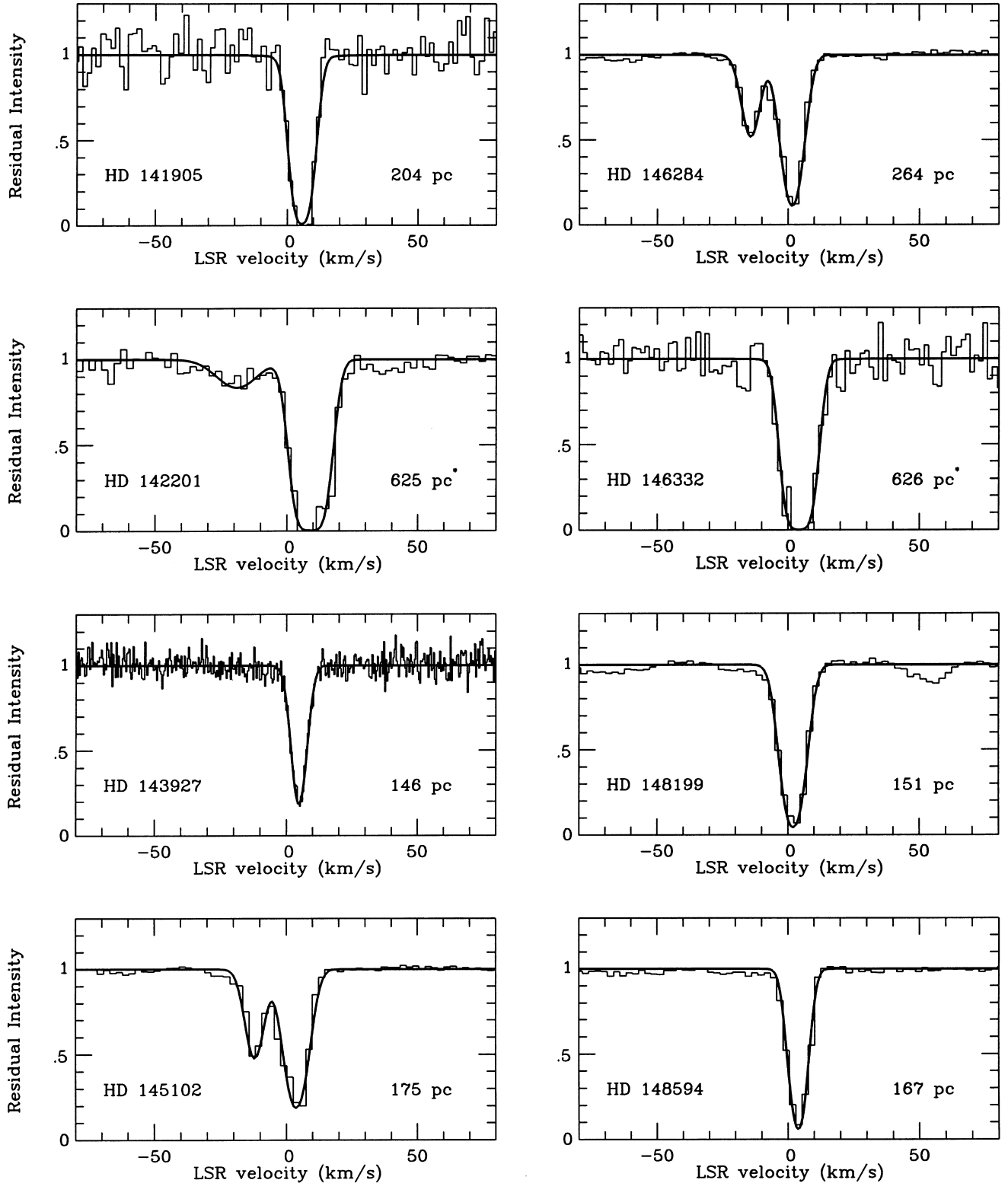


Figure 2 – continued

and is less than the overall size of Lupus 1 as mapped in ^{13}CO by Tachihara et al. (1996). All four of these stars have well-determined distances in the range 120–130 pc (Table 1), and none have detectable interstellar NaI absorption. Thus, I conclude that the Lupus 1 region must have a distance greater than 120 pc, and probably greater than 130 pc.

Similarly, three stars (HD 143118, 143699 and 143927) lie between the Lupus 2 ($l \approx 338^\circ$, $b \approx +12^\circ$) and Lupus 3 ($l \approx 340^\circ$, $b \approx +9^\circ$) regions, again within approximately 1° of either one or both of them. Of these three stars, a strong NaI line is present towards HD 143927 (146^{+22}_{-17} pc), but only upper limits were obtained for HD 143118 (151^{+20}_{-16} pc) and HD 143699

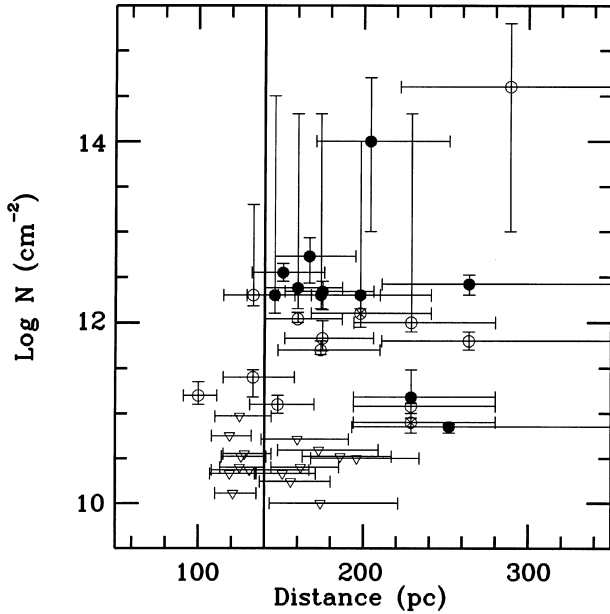


Figure 3. Column densities of the interstellar lines as a function of stellar distance, for those stars where the latter quantity is well defined. Filled circles represent absorption components with LSR velocities in the range ($0 < V_{\text{LSR}} < 12 \text{ km s}^{-1}$) occupied by the Lupus molecular clouds (Murphy et al. 1986). Open circles represent components with negative LSR velocities, while the two components represented by circumscribed crosses are the only examples towards these relatively nearby stars with LSR velocities more positive than the range occupied by the Lupus clouds (although two more distant stars also have such positive velocity components). Column density upper limits are represented by open triangles. Note that no stars having Lupus-like velocities occur closer to the Sun than 140 pc (vertical line).

Table 3. Published determinations of the distance to the Lupus molecular clouds. Based on the discussion of Krautter (1991), but revised and updated where appropriate (see text for discussion).

Method	Reference	Distance (pc)
Dist. to HR 5999/6000	ESA (1997)	223^{+35}_{-26}
Dist. to HD 143927	ESA (1997)	146^{+22}_{-17}
Extinction (~ 45 stars)	Franco (1990)	165 ± 15
Extinction (31 stars)	Hughes et al. (1993)	140 ± 20
Extinction (~ 250 stars)	Knude & Høg (1998)	100
Absorption lines (36 stars)	Present work	150 ± 10

(162^{+23}_{-18} pc). Owing to the range of errors on the stellar distances, the interpretation here is somewhat less clear-cut, although these observations are clearly best reconciled for a distance of ~ 150 pc to the absorbing medium (a distance as low as 100 pc would certainly result in all three stars having strong interstellar absorption lines). In any case, a distance as low as 100 pc seems to be excluded by the non-detection of interstellar lines towards HD 142431 (119^{+13}_{-11} pc), which lies only $\sim 3^\circ$ south of Lupus 2, and approximately midway between Lupus 2 and Lupus 4 (cf. fig. 1b of Krautter 1991, or ESO Sky Survey field 330).

The present results therefore strongly suggest that the distance of 100 pc to the Lupus complex obtained by Knude & Høg (1998) is a significant underestimate. The most likely explanation for this is the contribution of relatively low-density foreground material to the extinction of background stars. Such material is in fact known

to be present in this direction, where it occurs as a shell (or shells) of material flowing outwards from the Sco-Cen association (e.g. Weaver 1979; Crawford 1991; de Geus 1992). This material is quite evident in H I maps of the region (e.g. Colomb, Pöppel & Heiles 1980) and, being an outflow from the Sco-Cen association, it occurs at generally negative LSR velocities. Indeed, several such components may be identified in the present study (see below). As these components must necessarily lie in the foreground, any interstellar extinction associated with them will affect more nearby stars, leading to an underestimate of the distance to the Lupus molecular clouds if the latter are assumed to be the sole source of interstellar extinction in this direction.

4.2 The blueshifted components

Most of the interstellar absorption components with velocities outside the range occupied by the molecular clouds occur at negative LSR velocities (open circles in Fig. 3). Only one of these, that towards HD 139094, has a column density significantly in excess of $\log N = 12.00$. As noted above, the velocity of this component (-3.1 km s^{-1} ; Table 1) is only slightly outside the Lupus velocity range, and may in fact be associated with it. Moreover, the width of this highly saturated component is consistent with at least two unresolved components having LSR velocities close to -5.0 and 0.0 km s^{-1} , and may therefore plausibly be due to a Lupus component blended with a more blueshifted component.

The remaining blueshifted components have significantly lower column densities. As first noted by Crutcher (1982) and Frisch & York (1986), negative LSR velocities are commonly observed in this direction and, as discussed above, this is attributed to a general outflow of material from the Sco-Cen OB association (Crawford 1991; de Geus 1992). The negative velocity components observed here are therefore interpreted as arising in the Sco-Cen shell(s). Some of these components have Na I column densities as high as $\log N \approx 12.00$, which, according to the empirical relations between $N(\text{H})$ and $E(B - V)$ and $N(\text{Na I})$ and $N(\text{H})$ obtained by Bohlin, Savage & Drake (1978) and Ferlet, Vidal-Madjar & Gry (1985), would contribute a colour excess of $E(B - V) \approx 0.03$ mag. It is this contribution to the interstellar extinction that I suggest may have influenced the results of Knude & Høg (1998) discussed above.

4.3 The redshifted components

Four stars in the present sample were found to exhibit absorption components with $V_{\text{LSR}} > 12 \text{ km s}^{-1}$, i.e. greater than the velocity range occupied by the Lupus molecular clouds (although only marginally so in the case of HD 148703). It is notable that all four occur towards stars with distances ≥ 200 pc, and that the highest velocities ($V_{\text{LSR}} \approx +17 \text{ km s}^{-1}$) occur towards stars with (photometric) distances of ~ 400 pc (HD 139524 and 141180; Table 1). It therefore seems reasonably clear that on the far side of the Lupus complex, in the distance range 200–400 pc, there exists interstellar material that is moving away from the molecular clouds with a relative velocity of the order of 10 km s^{-1} . This velocity is in the wrong sense to be explained by Galactic rotation for this Galactic longitude, and the most plausible explanation is that these components arise in the *far* side of the Sco-Cen outflow, the near side of which is responsible for the blueshifted components discussed in Section 4.2.

4.4 The upper limits

Sixteen of the stars studied here (44 per cent) were found to have no detectable interstellar Na I absorption, with corresponding $\log N$ upper limits in the range 10.00 to 11.00, depending on the signal-to-noise ratios of the individual spectra. These upper limits are represented by open triangles in Fig. 3. On the basis of the discussion in Section 4.1 we might expect all these upper limits to occur towards stars closer than 150 pc, the estimated distance to the molecular clouds.

As it happens, while half of these upper limits are indeed found towards stars closer than 150 pc, and several others are consistent with such a distance given the *Hipparcos* distance errors, there nevertheless does appear to be a significant group of stars with distances ≥ 160 pc and $\log N \leq 10.50$. It is notable that, with the exception of HD 143699 (one of the stars discussed in Section 4.1), for which the *Hipparcos* errors would in any case permit a distance closer than 150 pc, all of these relatively distant stars lacking interstellar Na I occur to the south and west (lower l) of the molecular cloud complex (cf. Fig. 1). In contrast, stars at a similar distance (≈ 160 – 170 pc) but to the north and east (e.g. HD 141637, 145102 and 148594) do exhibit absorption components with velocities consistent with the molecular gas. This suggests that any outlying non-molecular gas associated with the Lupus complex (or the larger-scale ridge of giant molecular clouds of which it forms a part) lies 10–30 pc further away to the south and west of the molecular clouds than to the north and east. On the other hand, it is also possible that outlying gas does lie at the same distance as the molecular clouds, but has a patchy distribution not properly sampled by the relatively small number of stars observed here. Additional observations of foreground and background stars would be required to decide between these two possible interpretations.

5 CONCLUSIONS

The principal conclusions of the present work are as follows:

- (i) Based on the minimum distance at which strong interstellar Na I absorption lines appear in the spectra of stars observed towards the Lupus molecular clouds, I obtain a distance to the latter of 150 ± 10 pc.
- (ii) This is in good agreement with most other estimates of the distance to the Lupus clouds (Table 3), with the notable exception of the value of 100 pc obtained recently by Knude & Høg (1998). I have suggested that their interstellar extinction data may have been biased by lower-density foreground material flowing outwards from the Sco-Cen OB association.
- (iii) Absorption components with velocities more positive than those expected for the Lupus clouds ($V_{\text{LSR}} > 12 \text{ km s}^{-1}$) are found towards several stars with distances greater than ~ 200 pc. I suggest that these may arise in the *far* side of the Sco-Cen shell(s), the near side of which is well known to produce blueshifted velocity components towards stars in this region of the sky.

- (iv) The distribution of stars on the sky with distances ≥ 160 pc but with $\log N \leq 10.50$ suggests that any non-molecular interstellar matter associated with the Lupus complex lies further from the Sun (by perhaps 10–30 pc) to the south and west of the molecular clouds than to the north and east.

ACKNOWLEDGMENTS

I thank the Mt Stromlo Observatory for many generous allocations of telescope time over the years, and PPARC for the award of an Advanced Fellowship. Mr Chuen-Man Chow assisted with certain aspects of this work as part of an undergraduate project at UCL.

REFERENCES

- Appenzeller I., Mundt R., Wolf B., 1978, *A&A*, 63, 289
 Barlow M. J., et al., 1995, *MNRAS*, 272, 333
 Bessell M. S., Eggen O. J., 1972, *ApJ*, 177, 209
 Bohlin R. C., Savage B. D., Drake J. F., 1978, *ApJ*, 224, 132
 Colomb F. R., Pöppel W. G. L., Heiles C., 1980, *A&AS*, 40, 47
 Crawford I. A., 1991, *A&A*, 247, 183
 Crawford I. A., Barlow M. J., Blades J. C., 1989, *ApJ*, 336, 212
 Crutcher R. M., 1982, *ApJ*, 254, 82
 Dame T. M., et al., 1987, *ApJ*, 322, 706
 de Geus E. J., 1992, *A&A*, 262, 258
 de Geus E. J., de Zeeuw P. T., Lub J., 1989, *A&A*, 216, 44
 Dunkin S. K., Crawford I. A., 1999, *MNRAS*, 302, 197
 Eggen O. J., 1983, *MNRAS*, 204, 377
 ESA, 1997, *The Hipparcos and Tycho Catalogues*. ESA SP-1200. ESA Publications Division, Noordwijk,
 Ferlet R., Vidal-Madjar A., Gry C., 1985, *ApJ*, 298, 838
 Franco G. A. P., 1990, *A&A*, 227, 499
 Frisch P. C., York D. G., Smoluchowski R., Bahcall J. N., Matthews M. S., 1986, *The Galaxy and the Solar System*, Univ. Arizona Press, Tucson, p. 83
 Hobbs L. M., 1969, *ApJ*, 157, 165
 Hobbs L. M., 1978, *ApJ*, 222, 491
 Howarth I. D., Murray J., Mills D., Berry D. S., 1998, *Starlink User Note* 50.21,
 Hughes J., Hartigan P., Clampitt L., 1993, *AJ*, 105, 571
 Knude J., Høg E., 1998, *A&A*, 338, 897
 Krautter J., Reipurth B., 1991, *Low Mass Star Formation in Southern Molecular Clouds*, ESO Scientific Report 11, p. 127
 Morton D. C., 1991, *ApJS*, 77, 119
 Murphy D. C., Cohen R., May J., 1986, *A&A*, 167, 234
 Perryman M. A. C., et al., 1997, *A&A*, 323, L49
 Schneider S., Elmegreen B. G., 1979, *ApJS*, 41, 87
 Shortridge K., et al., 1998, *Starlink User Note* 86.16,
 Somerville W. B., 1988, *Observatory*, 108, 44
 Stapinski T. E., Rodgers A. W., Ellis M. J., 1981, *PASP*, 93, 242
 Tachihara K., Dobashi K., Mizuno A., Ogawa H., Fukui Y., 1996, *PASJ*, 48, 489
 Wallace P. T., Clayton C. A., 1996, *Starlink User Note* 78
 Weaver H., 1979, in Burton W. B., ed., *Proc. IAU Symp. 84, The Large Scale Characteristics of the Galaxy*. Reidel, Dordrecht, p. 295
 Welty D. E., Hobbs L. M., Kulkarni V. P., 1994, *ApJ*, 436, 152

This paper has been typeset from a \LaTeX file prepared by the author.